Estimating 3D Fibre Process Anisotropy

MARCELA HLAWICZKOVÁ, [1] PETR PONÍŽIL, [2] IVAN SAXL
Department of Probability and Statistics, Charles University
Sokolovská 83, CZ 186 75, Praha 8, Czech Republic
[1] Department of Physics and Material Engineering, Tomas Bata University
Námì stí TGM 275, CZ-762 72 Zlín, Czech Republic
[2] Mathematical Institute, Academy of Sciences of the Czech Republic
Žitná 25, CZ 115 67 Praha 1, Czech Republic

Abstract: The method of the Steiner compact is used to estimate the anisotropy of several random spatial fibre processes generated by simulations and representing a continuous passage from a pronounced anisotropy to the complete isotropy. Three anisotropic fibre processes with atomic measures are also considered for the comparison.

Key-Words: anisotropy, rose of directions, zonotope, fibre process, Prohorov distance

1 Introduction

Many features of examined natural and artificial objects (blood vessels, nerves, rivers, geological faults, rod- and fibre-like strengthening particles, drainage, traffic routes etc.) have one strongly prevailing size. Their understanding requires the estimation of their length and orientation. The stochastic models of such features are fibre processes $\boldsymbol{L}$, i.e. random closed sets of one-dimensional segments arranged in space [1]. If they are stationary, their main characteristic is the intensity L defined by $\mathbf{E}h_1(\boldsymbol{L} \cap B) = L\nu(B)$, where B is a bounded Borel set (sampling probe), $\nu(\bullet)$ is the Lebesgue measure and $h_1(\bullet)$ is the Hausdorff measure. The orientation distribution is described by the directional distribution P (rose of directions), which is an even probability measure on the unit sphere $S^{d-1} \subset \boldsymbol{R}^d$. P can be interpreted as the distribution of tangents at a typical point of the stationary random fibre set generated by the process.

The frequently used method of estimating P consists in the examination of point processes $\Phi(u_i)=\boldsymbol{L}\cap F_i$, i=1,2,…, where F_i are hyperplanes with normals u_i. The d-dimensional problem is thus reduced to a (d-1)-dimensional estimation, which is an approach typical for stereology.

To estimate the rose of directions, the geometrical approach can be used based on zonotopes and zonoids (limits of zonotopes with respect to the Haussdorff metric). A convex body is a zonoid K if and only if its support function is

$$h(K;u) = \int_{S^{d-1}} \left|\langle v,u\rangle\right| r_K(\mathrm{d}v) \qquad (1)$$

for all $u \in S^{d-1}$, where ρ_K is a positive even measure and $\langle,\rangle$ stands for an ordinary scalar product [2].

A special situation arises when the generating function ρ_K is an atomic measure concentrated on a finite collection of directions v_j, i=1,2,…,m. Eq. (1) then degenerates to a sum

$$h(Z_m;u) = \sum_{j=1}^{m} \left|\langle v_j,u\rangle\right| a_j, \qquad (2)$$

where α_j are the weights and Z_m is a centred convex body with centred faces called the zonotope, which is a finite sum - in the sense of Minkowski - of centred line segments $\alpha_j[-v_j,v_j]$.

A similar situation is encountered in the case of a fibre process of intensity L. Let $\theta(u_i)$ be the intensity of $\Phi(u_i)$ (assuming that Φ is stationary). It is related to P just by the equation (1) (s.c. cosine transformation formula) when replacing h by θ and ρ by LP. Consequently, the anisotropy of $\boldsymbol{L}$ can be in principle described by a zonoid Z (called the Steiner compact) with the generating function LP.

In $\boldsymbol{R}^2$, the knowledge of a finite number of support function values $\theta(u_i)$, i=1,…,n, makes the construction of a centred symmetric body Z_n with $h(Z_n; u_i)= h(Z; u_i)$ possible and it can be used to estimate P [3]. The situation is somewhat different in $\boldsymbol{R}^3$ [2], however, even here exists a zonotope Z_m, $m \geq n$, with the property that the values of its support function $h(Z_m; u_i)$ equal the values of the support function $\theta(u_i)$ of the zonoid Z with the generating function P. The zonotope Z_m may be estimated from the values $\theta(u_i)$ [4] and its generating function P_m is the estimate of the rose of directions P. The

distance between the two measures P, P_m can be measured using the Prohorov distance (see [4,5]).
The arc and polyhedral test systems for the anisotropy estimation in $\boldsymbol{R}^2$ were proposed in [5,6]. In order to transpose this idea to $\boldsymbol{R}^3$, polyhedral probes can be used. Three isotropic fibre processes (edges of various Voronoi tessellations) were examined by means of cubic and octahedral probes and the distribution of the Prohorov distance was estimated in [7]. Its variance decreases with the number of probe faces (similarly as with the number of random testing planes [4]) and increases with a growing local inhomogeneity of the process as characterized e.g. by the distribution of the cell volume.

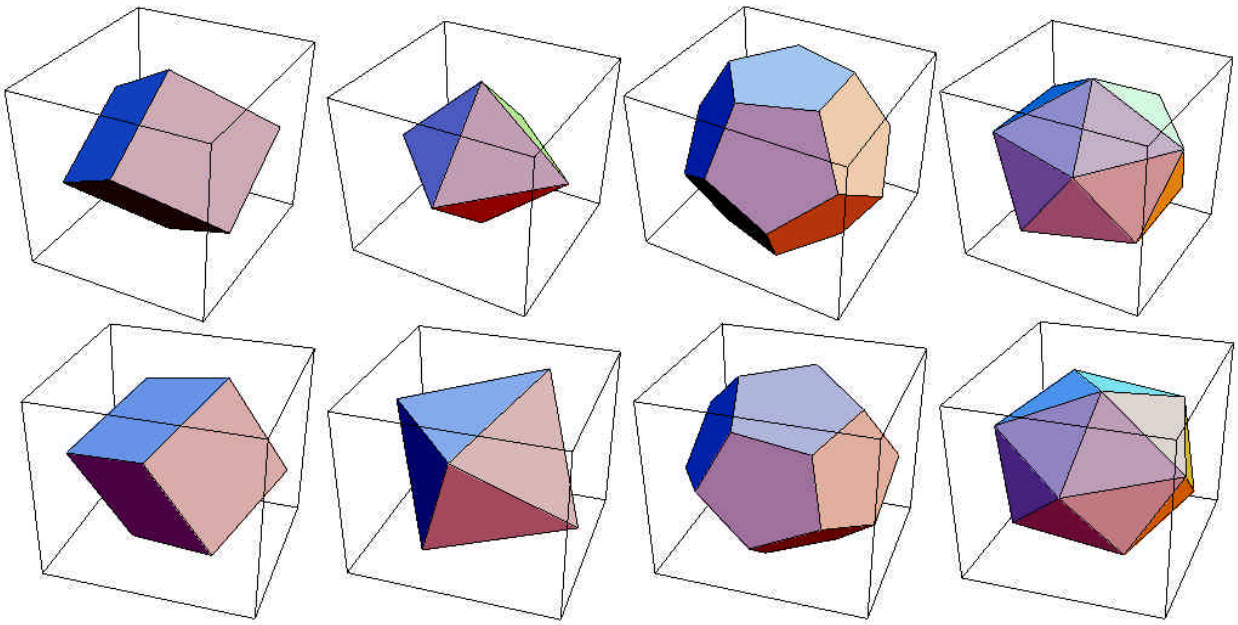

Fig. 1 Probes in the Ω_0 (upper row) and Ω (lower row) orientations.

In the present study, random spatial fibre processes - again the processes of Voronoi cell edges - are examined by means of four different polyhedral probes. The processes represent a continuous passage from a pronounced anisotropy of linear and planar types to the complete isotropy and, beside processes with diffuse anisotropy measure, also three processes with atomic measures are considered for the comparison.

2 Results

2.1 Examined fibre processes

i) The monoclinic point lattice $\boldsymbol{H}_0$ with the lattice vectors $|a_1|=|a_2|=|a_3|/q$, $\langle a_1,a_2\rangle=0.5|a_1|^2$ generates the *isohedral tiling* $\boldsymbol{T}_0$ of the space by regular hexagonal prisms with the base formed by pairs of three edges v_1, v_2, $v_3= -v_1 -v_2$ of equal lengths b, and six vertical edges $|v_4|=qb$. The edge process $\boldsymbol{L}_0(q)$ with atomic measures was examined in three particular cases: thin plates (q=0.2), equiaxial hexagonal prisms (q=1) and long rods (q=10), the orientation of the v_2 and v_4 edges were $\{0,b,0\}$, $\{0,0,qb\}$, respectively.

ii) Let ξ_x be i.i.d. random vectors with the normal $N(0,\Xi^2)$ distribution, $\Xi^2=a^2\boldsymbol{I}$, $\boldsymbol{I}$ is a unit matrix and $x \in \boldsymbol{H}_0$ denotes the lattice points. The *displaced lattice* or the *Bookstein model* on $\boldsymbol{H}_0$ [8] is then $\boldsymbol{H}_a = \bigcup_{x\in \boldsymbol{H}_0} (x+x_x)$. The tessellation $\boldsymbol{T}_a$ generated by $\boldsymbol{H}_a$ is a normal (two neighbouring cells have one common face, three cells meet along one edge and four cells meet in a vertex) random tessellation. Then also a relation between the mean cell perimeter $\mathbf{E}p$ (p is the total cell edge length) and the mean cell breadth $\mathbf{E}w$ holds: $\mathbf{E}p=12\mathbf{E}w$. The edge process $\boldsymbol{L}_a(q)$ with a diffuse anisotropy measure was examined for a=0.005, 0.2, 0.5, 2 (in the units of the nearest neighbour distance in $\boldsymbol{H}_0$) at the values of q chosen above for $\boldsymbol{L}_0(q)$. For high a, $\boldsymbol{T}_a$ approaches the stationary Poisson-Voronoi tessellation and $\boldsymbol{L}_a$ is isotropic.

In a normal random edge process $\boldsymbol{L}_a$, each cell contribute to the process intensity L_a by $\mathbf{E}p/(3\mathbf{E}v)=4\mathbf{E}w/\mathbf{E}v$, where v is the cell volume. In contrast to $\boldsymbol{T}_a$, $\boldsymbol{T}_0$ is not normal; v_4 edges are three-valent, base edges are four-valent. The weights of the fibre orientations are $\alpha_1=\alpha_2=\alpha_3=\alpha=(3+2q)^{-1}$, $\alpha_4=2q\alpha$ and the cell contribution to the intensity L_0 is $b\alpha^{-1}/v < (1+\alpha^{-1})b/v = p/(3v)$ ($b=[4/(27q^2)]^{1/6}$ in the unit v=1 tiling).

Hence the intensity $L_a(q)$ is discontinuous at $a \to 0_+$. Even the smallest point shifts in the generating $\boldsymbol{H}_0$ lattice evoke a substantial increase (the higher the smaller is q) in $L_a(q)$ and other tessellation characteristics like are the mean number of edges per cell $\mathbf{E}n_e$ and the $\mathbf{E}p/\mathbf{E}w$ ratio - see Tab. 1.

Tab. 1. Characteristics of unit tilings $\boldsymbol{T}_0(q)$ and random tessellations $\boldsymbol{T}_a(q)$, a=0.005.

	$\boldsymbol{T}_0(q)$	$\boldsymbol{T}_a(q)$	$\boldsymbol{T}_0(q)$	$\boldsymbol{T}_a(q)$	$\boldsymbol{T}_0(q)$	$\boldsymbol{T}_a(q)$	$\boldsymbol{T}_0(q)$	$\boldsymbol{T}_a(q)$	$\boldsymbol{T}_0(q)$	$\boldsymbol{T}_a(q)$
q	n_e	$\mathbf{E}n_e$	L	L	p/L	$\mathbf{E}p/L$	w	$\mathbf{E}w$	p/w	$\mathbf{E}p/\mathbf{E}w$
0.2	18	42.0	4.23	7.96	3.88	3	1.99	1.99	8.25	12.00
1.0	18	41.3	3.64	5.81	3.60	3	1.45	1.45	8.99	12.00
10.0	18	36.9	7.77	8.73	3.12	3	2.19	2.18	11.03	12.00

2.2 Simulations and polyhedral probes

The tessellations have been constructed in a unite cube by means of the incremental method with the nearest neighbour algorithm [9]. The number of process realizations was between 500 and 1000.

Four centrally symmetric polyhedral probes of the same surface area (A = 0.8617) have been placed in the centre of the tessellated unit cube - Fig.1. In order to suppress a possible positional bias between the tessellation and the probes, each realization was randomly shifted as a whole with respect to the cube centre by a random vector η with the normal $N(0,\Xi^2)$ distribution, $\Xi^2=\tau^2\boldsymbol{I}$ and the value of τ was comparable with the lattice constants of $\boldsymbol{H}_0$.

Two orientations of the probes were examined, namely Ω_0 (cube diagonal perpendicular to the $\{x,y\}$ - plane and two edges parallel to the x-axis, all octahedron diagonals parallel to the coordinate axes, two dodecahedral faces perpendicular to the z-axis and two dodecahedral edges parallel with the x-axis, one icosahedral diagonal perpendicular to the $\{x,y\}$ - plane and two icosahedral edges parallel with the x-axis), and Ω obtained by rotations from Ω_0 (cube and octahedron rotated by Euler angles $(\phi,\psi,\chi)=(\pi/7,\pi/3,\pi/2)$, dodecahedron and icosahedron rotated by $(\pi/7,\pi/9,\pi/2)$) - see Fig. 1. Their size and the intensities of tessellations λ were chosen in such a way that the expected total number of intersections per the whole probe $\mathbf{E}N$ was approximately constant ($\mathbf{E}N$=1840) in all considered cases and the edge effects were considerably suppressed by confining the examination to the central part of the unit cube.

The estimation error was quite negligible, but the observed values $\mathbf{E}N$(obs) were biased by the specific probe orientations - Tab. 2. The bias is appreciably reduced even by averaging the two different probe orientations Ω_0, Ω only.

Tab. 2. The ratios $\mathbf{E}N$(obs)/$\mathbf{E}N$; a=0.005.

q	$cube_{\Omega 0}$	$cube_{\Omega}$	$oct_{\Omega 0}$	oct_{Ω}	$dod_{\Omega 0}$	$icos_{\Omega}$
0.2	1.09	0.98	1.05	0.95	1.06	0.97
1.0	1.10	1.00	1.08	0.96	1.09	1.03
10	1.14	1.03	1.13	0.96	1.13	1.04

2.3 Estimation of the rose of intersections

Let u_i, i=1,…,n, n=6,8,12,20, be the known unit normals of the probe faces. The intersection number intensities N_i/A at the individual faces of n-hedral probes are estimates of the support function values $h(\bullet, u_i)$ of the zonoid $Z_a(q)$ characterizing the fibre process anisotropy. The processes $\boldsymbol{L}_a$, $\boldsymbol{L}_0$ differ in their intensities (Tab. 1) and certain difference in the orientation anisotropy is also unavoidable. Consequently, the comparison of the support function $h_0(Z_4, u_i)$ of the zonotope Z_4 (generated by line segments $\alpha_i[-v_i, v_i]$, i=1,…,4, see Eq. (2)) and estimated values $h_a(Z_a, u_i) \propto \theta(u_i)$ gives the first information concerning this difference; the small values of a are particularly important.

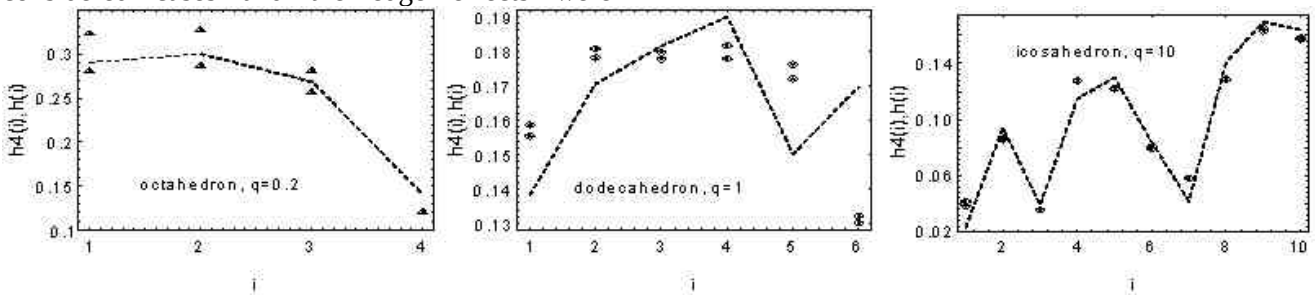

Fig. 2 The theoretical values of the normalized support function $h4(i)$ (vertices of the dotted curves) and the estimated values of $h(i)$ in the directions of the probe face normals u_i at various values of q (the vertical point pairs correspond to the antipodal probe faces).

Multiplying the support function by an arbitrary non-zero constant does not change the shape of the convex body in question, hence the normalized sets of theoretical and estimated support function values $h4(i)=c.h(Z_4,u_i)$, $h(i)=c'.N(i)$, $\sum_{i=1}^{n} h4(i) = \sum_{i=1}^{n} h(i) = 1$, have been compared - Fig. 2. In agreement with Tab. 1, the difference between the support functions is more pronounced at lower values of q.

2.4 Estimation of the rose of direction

The zonotope Z_m approximating the zonoid Z of the examined fibre process $\boldsymbol{L}$ is estimated by the maximum likelihood (ML) procedure proposed in [4]. Z_m is the sum of centred line segments $\beta_j[t_j,-t_j]$, where $t_j \in T = \{t_1,\ldots,t_m, -t_1,\ldots,-t_m\}$, $m=n(n-1)/2$. T is the union of normalized (unit) alternating products of the probe face normals u_i, $i=1,\ldots,n$. The discretized ML problem consisting in the estimation of the weights β_i is solved by the iteration EM algorithm (see [4]).

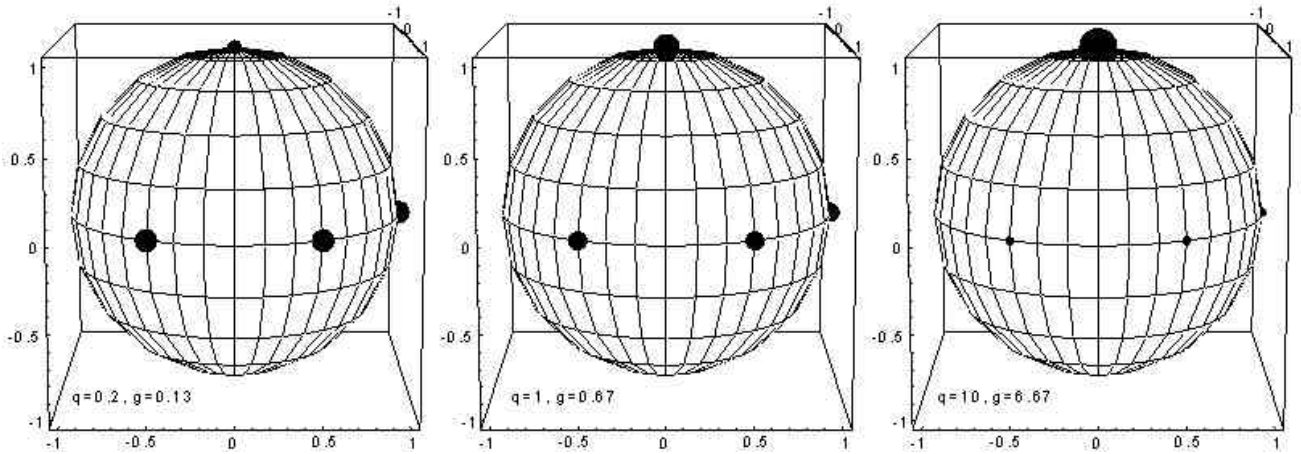

Fig. 3 Orientations and weights in $\boldsymbol{L}_0$ fibre (edge) processes.

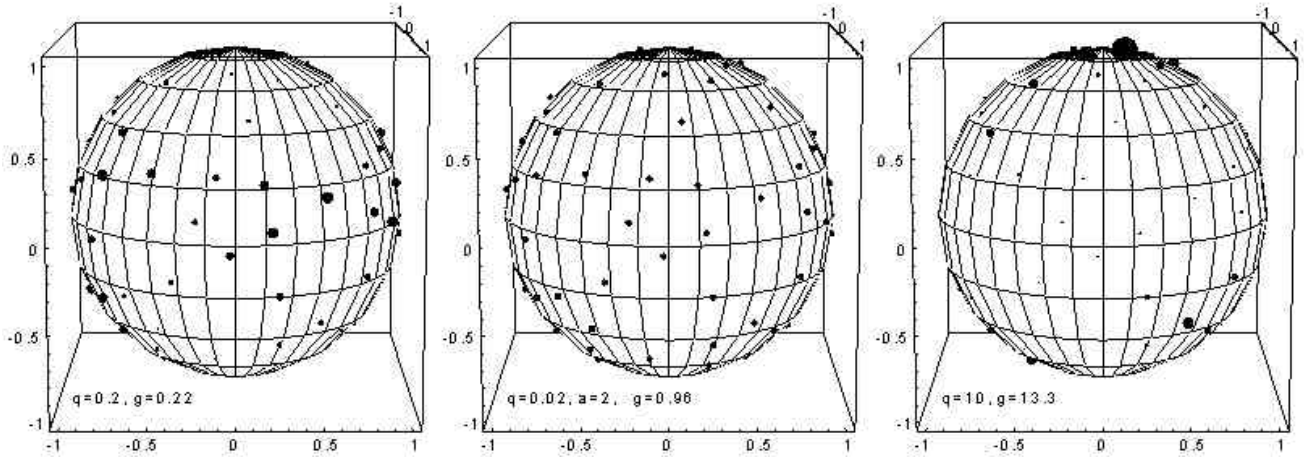

Fig. 4 Orientations and weights in $\boldsymbol{L}_{0.005}$ (left and right figure) and in $\boldsymbol{L}_2$ fibre processes (middle figure) at various values of q as estimated by icosahedral probes in the orientation Ω.

The atomic measures of $\boldsymbol{L}_0$ are shown in Fig. 3, positions and weights of the directions generating $\boldsymbol{Z}_{45}$ as estimated by icosahedral probes are presented in Fig. 4 (the circle areas are proportional to the weights α_i, β_i; their total area is 1% of the projected sphere area). Even a simple visual inspection of Fig. 4 reveals the strong concentration of atomic measures in the equatorial strip at q=0.2 and near the pole at q=10. Other probes give similar but less detailed results (Fig. 5). A simple numerical characteristic of measure arrangement and strength is the ratio

$$g = \sum_{i|t_i \in T \setminus T_1} b_i \Big/ \sum_{j|t_j \in T_1} b_j \qquad (3)$$

where $T_1=\{t_i|\langle t_i,z\rangle \geq 0.5\}$ is the subset of atomic measures lying in the equatorial strip of the area 2π. For $\boldsymbol{L}_0$, $g=3/(2q)$, whereas $g \approx 1$ in the isotropic case. The gradual establishment of isotropy with growing a demonstrates Fig. 6a; probes with higher face numbers give more accurate estimates of g.

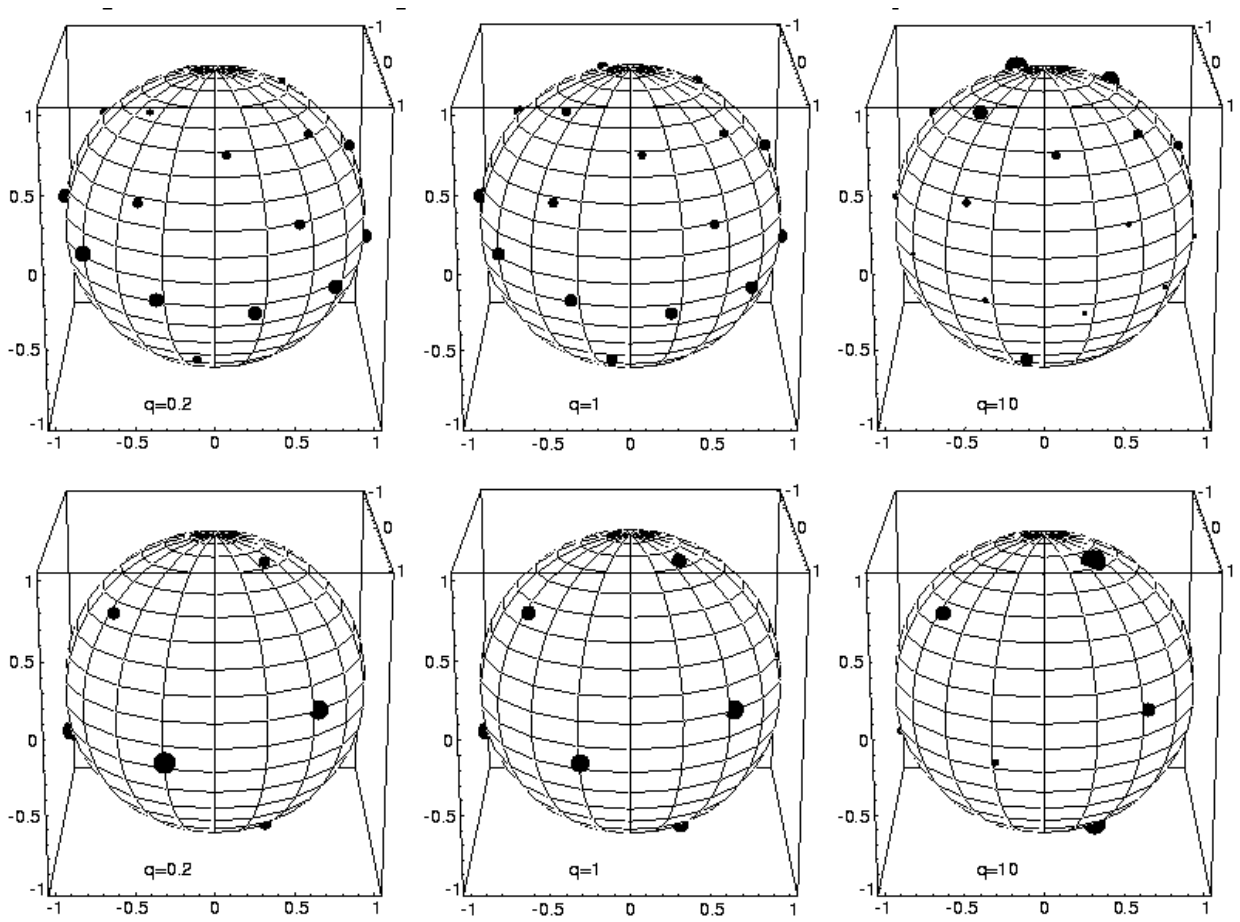

Fig. 5 Orientations and weights in $\boldsymbol{L}_{0.005}$ fibre process at various values of q as estimated by dodecahedral (upper row) and octahedral (lower row) probes in the Ω orientations. Note the gradually decreasing information content in comparison with Fig. 4.

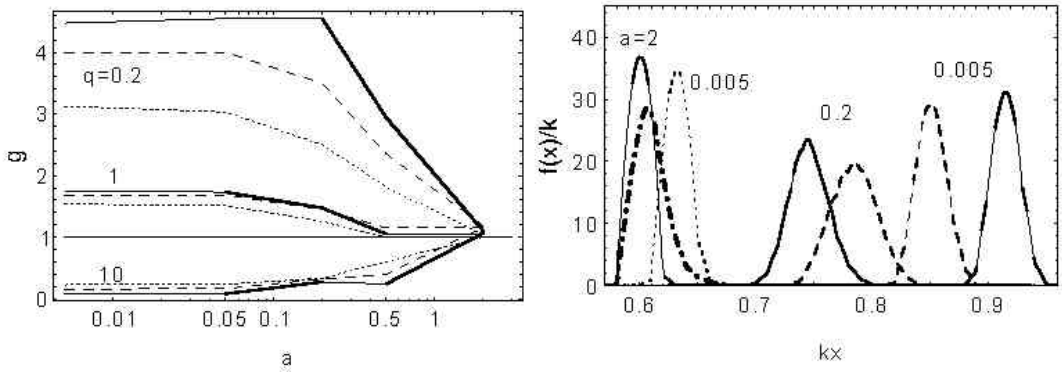

Fig. 6 Anisotropy characteristics of the process $\boldsymbol{L}_a$. (a) The parameter g estimated by icosahedral (full line), dodecahedral (dashed) and octahedral (dotted) probes in the Ω orientations. (b) The pdf of the Prohorov distance $d(P_6,P)$ as determined by the octahedral probe for q=0.2 (dashed), 1 (dotted), 10 (full line) and for the edge process of the Poisson-Voronoi tessellation as estimated in [7] (thick dash-dotted line) – k=2π.

This approach to the isotropy can also be followed by estimating the Prohorov distance $d=d(P_m, P)$ between the probability measures P_m (related to the zonotop Z_m) and P=1/4π (corresponding to the isotropy describing sphere). The estimates of the pdf of d are shown in Fig. 6b (the Epanechnikov kernel estimator was used). Whereas the standard deviations of distance distributions are comparable ([0.027,0.032] is the observed range of values), their mean values are proportional to the degree of the fibre anisotropy. A more detailed account of the present results will be published elsewhere.

3 Conclusion

The presented comparison of results obtained by simulation and implied by theory demonstrates the possibilities of the Steiner compact approach to the anisotropy characterization in $\boldsymbol{R}^3$; in particular the various polyhedral probes are compared and an application of the Prohorov distance estimation is shown. The higher is the number of probe faces the more accurate characteristics are obtained.

Acknowledgement: The research was supported by the Grant Agency of the Czech Republic (contract No. 201/99/0269) and by the Ministry of Education of the Czech Republic (contract No. 281100015 - P.P.).

References:

[1] D. Stoyan, W.S. Kendall, J. Mecke, *Stochastic Geometry and its Applications.* J. Wiley&Sons, New York, 1995.

[2] P. Goodey, W. Weil, W. In P.M. Gruber, J.M. Wills (eds.):*Handbook of Convex Geometry*, North Holland, Amsterdam 1993, p. 1297.

[3] J. Rataj, I. Saxl, Analysis of Planar Anisotropy by Means of the Steiner Compact. *J. Appl. Prob.* Vol. 26, 1989, No. XX, pp. 490 - 502.

[4] M. Kiderlen, Non-Parametric Estimation of the Directional Distribution of Stationary Line and Fibre Processes. *Adv.Appl. Prob.*, Vol. 33, 2001, No. 1, pp. 6 - 24.

[5] V. Beneš, A. Gokhale, Planar Anisotropy Revisited *Kybernetika*, Vol. 36, 2000, No. 2, pp. 149 - 164.

[6] V. Beneš, M. Hlawiczková, A. Gokhale, G.F. VanderVoort, Anisotropy Estimation properties for Microstructural Properties. *Materials Characterization*, Vol. 46, 2001, No.2-3, pp. 93 - 98.

[7] M. Hlawiczková, Estimating Fibre process Anisotropy, In: *Proc. Conf. Inversion Problems*, March 2001, Aalborg University (in press).

[8] D. Stoyan, H. Stoyan, *Fractals, Random Shapes and Point Fields*, J. Wiley&Sons, New York, 1994.

[9] A. Okabe, B. Boots, K. Sugihara, *Spatial tessellations*, J.Wiley&Sons, Chichester, 1992.